Molecular Simulation of the Nanoscale Water Confined between an Atomic Force Microscope Tip and a Surface

H. J. Choi[*], J. Y. Kim[*], S. D. Hong[*], M. Y. Ha[*], and J. Jang[**]

[*]Department of Mechanical Engineering, Pusan National University, Busan 609-735, Korea
[**]Department of Nanomaterials Engineering, Pusan National University, Miryang 627-706, Korea,
jkjang@pusan.ac.kr

ABSTRACT

Under ambient humidity, water condenses as a meniscus between an atomic force microscope (AFM) tip and a surface, giving rise to a strong capillary force on the tip. We performed a molecular dynamics simulation of the nano-confined water meniscus. We studied the effects of the tip and surface hydrophilicity on the meniscus structure. By changing the tip-surface distance, we have simulated the formation, shrinkage, and breakage of the water meniscus. The nanometer meniscus substantially fluctuates in its periphery due to its instability, in agreement with our previous lattice gas simulation. We obtained the density profile and contact angle of the meniscus. By using these structural parameters, we calculated the capillary force between the tip and surface. Our calculation reproduced the typical behavior of the experimental force-distance curve.

Keywords: water meniscus, capillary force, AFM, molecular dynamics simulation

1 INTRODUCTION

Water naturally condenses between an atomic force microscope (AFM) tip and a surface under ambient conditions. This nanoscale water meniscus gives rise to a significant adhesion force on the order of nanonewtons which must be supplied to retract an AFM tip contacting a surface [1] (so called pull-off force). This meniscus also serves as a nano-channel for molecules to flow from the tip to a substrate in dip-pen nanolithography [2]. Considering the widespread applications of the AFM tip in surface science and nanolithography, it is important to understand the meniscus and the resulting capillary force at the molecular level.

Previously, we have performed Monte Carlo simulations based on a lattice gas model [3,4]. We have explored the roles of surface roughness and hydrophilcity on the capillary force. This coarse grained model, although successful in capturing the qualitative features of the meniscus, cannot provide the full molecular details of the water meniscus. Herein, in order to gain molecular insights on the nanoscale meniscus, we have performed all-atom type molecular dynamics (MD) simulation. We study the molecular features of the water meniscus by examining the density profile of water and its variation as the tip retracts from a surface. We also calculate the capillary force by combining the thermodynamic theory and the structural parameters of the meniscus obtained from the molecular density profile.

2 SIMULATION DETAILS

We use the TIP3P model [5] for water-water intermolecular interaction potential. In this model, three atom-centered point charges (-0.834 on O and +0.417 on H) interact with each other through the Coulomb potential. The oxygen-oxygen interaction has an additional Lennard-Jones (LJ) potential, $U(r) = 4\varepsilon\left[\left(\sigma/r\right)^{12} - \left(\sigma/r\right)^{6}\right]$ [6]. The LJ parameters ε and σ of oxygen are 0.1521 kcal/mol and 0.35365 nm, respectively. Water molecule is taken to be rigid: the oxygen-hydrogen bond length is 0.09572 nm and the angle between two O-H bonds is 104.52°. The particle-mesh Ewald method with a grid spacing of 0.1 nm [7] is used to calculate the long-range electrostatic interactions between partial charges.

We assume both the AFM tip and surface are made of LJ atoms. The tip geometry is taken to be a hemispherical shell of atoms. To construct the tip, we initially set up a face-centered cubic (FCC) crystal with a lattice spacing equal to 0.321 nm (similar to the LJ σ parameter of carbon). Then we choose lattice points closest to the hemispherical surface with a radius of 13 nm. The resulting AFM tip is made up of 8212 atoms. The surface structure is similarly generated by picking up the top two layers of FCC with the same lattice spacing as the tip. The surface is composed of 4976 LJ atoms. Total of 1906 water molecules are initially positioned regularly (as a cubic lattice) between the AFM tip and surface. The simulation box has a size of 7.5 nm by 7.5 nm by 8.0 nm.

We apply the periodic boundary conditions in the directions parallel to the surface. We use the velocity Verlet algorithm for the propagation of MD trajectories [6]. We use the SHAKE [6] algorithm to keep water molecules rigid. Temperature was held constant (300K) by applying Langevin dynamics [8] method with a damping coefficient of 5 ps^{-1}. The time step is taken to be 1 fs and the typical length of MD trajectory is 0.5 ns. We have studied the formation, shrinkage, and breakage of the water meniscus by varying the distance between the AFM tip and surface from 1.4 nm to 4.2 nm with an increment of 0.1 nm. In

addition, we have systematically varied the water-tip and water-surface interaction energies. That is, we have considered two LJ epsilon values for the tip atom, ε_T =0.1 and 2.5 kcal/mol. The case of ε_T =0.1 kcal/mol can be thought to correspond to a hydrophobic tip because it is smaller than the LJ epsilon parameter (0.1521 kcal/mol) of water-water interaction. The tip with ε_T =2.5 kcal/mol can be called hydrophilic. The LJ epsilon parameter of the surface, ε_S, is varied as 0.1, 0.5, 1.0, 2.0, and 2.5 kcal/mol. As for the tip, the surface with ε_S =0.1 kcal/mol can be considered as a hydrophobic surface. All the other tips correspond to hydrophilic surfaces. The LJ interactions between a tip atom and water and between a surface atom and water are calculated by using Lorentz-Bertholet mixing rule [6].

3 RESULTS

Figure 1 shows the simulated water menisci for two different tip-surface distances. In this hydrophilic tip-hydrophilic surface case (both ε_S and ε_T are 2.0 kcal/mol), the meniscus has a concave shape at all the tip-surface distances. The meniscus neck reduces in width as the tip-surface distance increases from 1.4 nm to 3.7 nm. Also, notice the concave curvature of the water meniscus decrease in magnitude as we increase the distance between the AFM tip and the surface.

By collecting MD snapshots like in figure 1 and averaging them, we can calculate the density profile defined as the average number of water molecules at a given position. The density profile ρ is assumed to be cylindrically symmetric so that it is a function of the horizontal distance from the tip center, r, and the height from the surface, h. The initial 0.4 ns of MD trajectory is thrown out for equilibration, and MD snapshots after 0.4 ns are collected for the calculation of the density profile. The density profile is normalized in the sense that its highest value is scaled to be one. The bin sizes of the density profile in the horizontal and vertical directions, dr and dh, are 0.25 nm and 0.15 nm, respectively. Such a density profile is drawn for two tip-surface distances in figure 2. The contour line with a density of half is drawn as a dashed line. Then, assuming the meniscus periphery is a circle, we determined the radius r_1 and the center position of the circle by using the least-squares fitting of the concave part of the half-density contour line.

Figure 2 illustrates how the density profile changes as we vary the tip-surface distance from 1.6 nm to 3.7 nm. Since both the tip and the surface are hydrophilic ($\varepsilon_T = \varepsilon_S$ =2.0 kcal/mol), the water meniscus has a concave shape. As the tip (drawn as a curved solid line) retracts from the surface (height of zero), the meniscus neck

narrows almost down to 1 nm in half width. Also notice that, for a given tip-surface distance, the density profile changes rather smoothly from a liquid value (=1) to a vapor value (=0). In other words, the meniscus periphery is not infinitely sharp as is often assumed in thermodynamic theories. Instead, the periphery is rather fuzzy due to the inherent thermal fluctuations at the nanoscale. Roughly, the periphery has a thickness of about half nanometer.
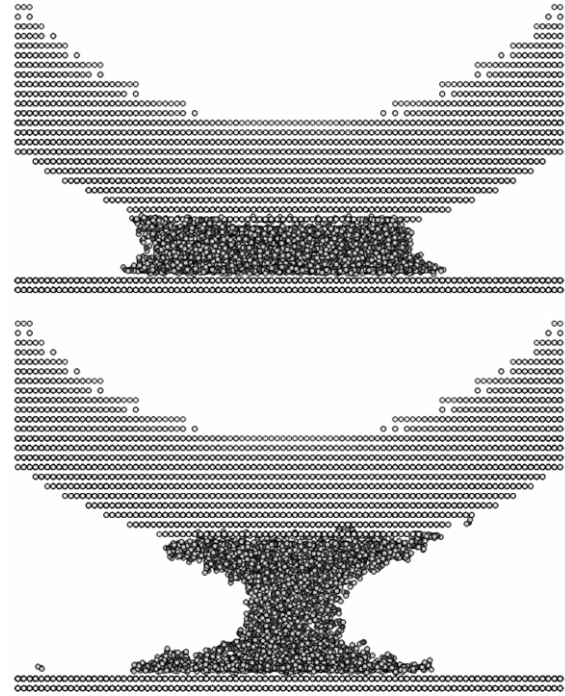

Figure 1: Simulated water menisci for two different tip-surface distances, 1.4 nm (top) and 3.7 nm (bottom). Both the tip and surface are hydrophilic.

Using the meniscus periphery obtained from the density profile, we can estimate the half-width of the meniscus neck r_2. Figure 3 shows how r_2 changes with an increase in the tip-surface distance. As expected, the half width in the neck decreases as the tip-surface distance increases up to the distance of 2.3 nm. As the distance becomes greater than 2.5 nm however, the meniscus half-width fluctuates, even though the overall trend is that the width decreases with raising the tip-surface distance. We think, due to the instability of the water meniscus at the distance over 2.5 nm, the water meniscus width varies rather irregularly.

With the structural parameters of meniscus (r_1 and r_2) obtained from the density profile, we can estimate the humidity of our simulation from the Kelvin equation,

$$RT \ln(p/p_0) = \gamma V \left(\frac{1}{r_1} + \frac{1}{r_2} \right), \qquad (1)$$

where γ and V are the surface tension (=0.076 N/m) and the molar volume (=1.8×10^{-5} m^3/mol) of water. R is the universal gas constant, T, the absolute temperature, p_0 the normal vapor pressure of the liquid, and p the pressure. The sign of r_1 is positive for a concave meniscus but negative for a convex one.
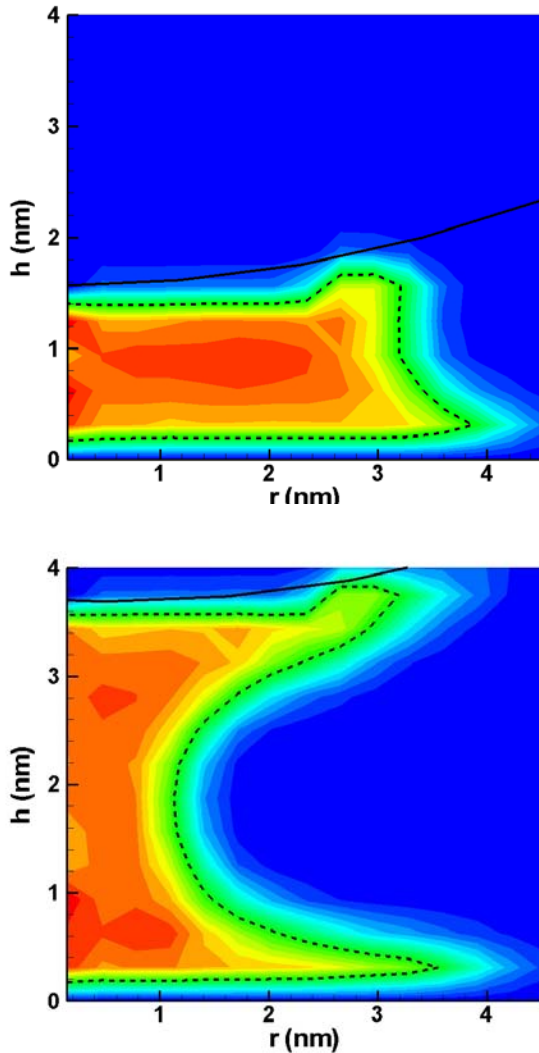

Figure 2: Change in the density profile of the water meniscus as the tip retracts from the surface. For a hydrophilic tip and a hydrophilic surface, the tip-surface distance is varied from 1.6 nm (top) to 3.7 nm (bottom).

The humidity calculated from equation (1) varies by changing the tip-surface distance, and it is found to vary from 60 to 70 percent. The capillary force F for a given tip-surface distance is given by

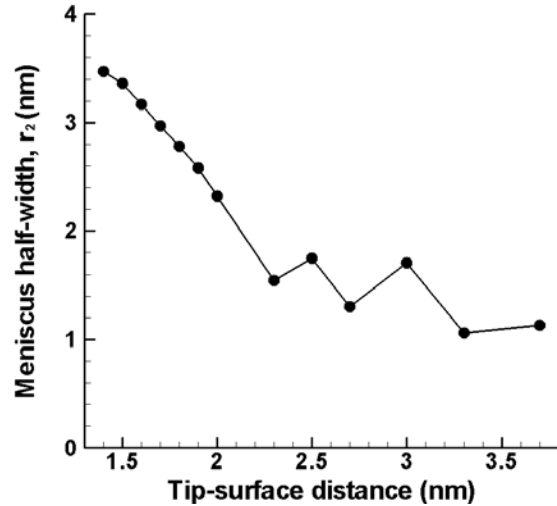$$F = \gamma \left(\frac{1}{r_1} + \frac{1}{r_2} \right) \times \pi r_2^2. \qquad (2)$$

Figure 3: The half-width at the meniscus neck, r_2, vs. the tip-surface distance. Both the tip and surface are hydrophilic (ε_T =2.0 kcal/mol, ε_S =2.0 kcal/mol).

Figure 4 shows the capillary force calculated from equation (2) vs. the tip-surface distance. The figure captures the essential features of a typical force–distance curve obtained in AFM experiment. The capillary force is most attractive at the shortest distance of our simulation, 1.4 nm, and it becomes less attractive as the tip-surface distance increases. At the distance of 3.3 nm, the force becomes zero due to the breakage of the meniscus.
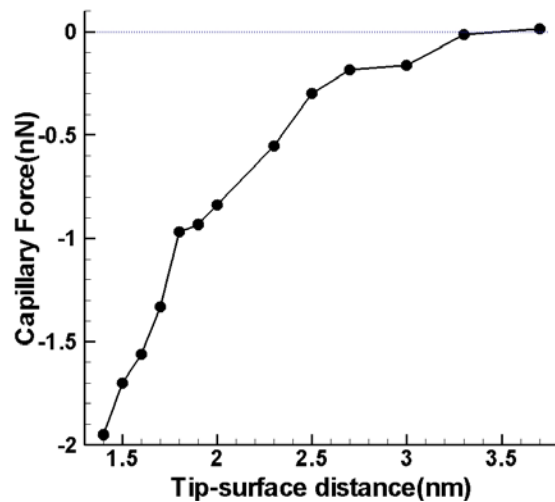

Figure 4: The capillary force as a function of the tip-surface distance. The tip and surface are both hydrophilic ($\varepsilon_T = \varepsilon_S$ =2.0 kcal/mol).

Figure 5 illustrates the effects of the surface hydrophilicity on the capillary force. The tip-surface distance is fixed to 1.5 nm. As the surface becomes more

hydrophilic with an increase in ε_S, the capillary force becomes more attractive. In the case of a hydrophobic tip (circles), the capillary force change its sign from positive (repulsive) to negative (attractive) at around ε_S =1.8 kcal/mol. As ε_S increases, an initially convex meniscus becomes a concave one, and the capillary force changes from repulsive to attractive. In the case of hydrophilic tip (triangles), the change in sign of the capillary force occurs at a lower value of ε_S (near 0.8 kcal/mol) than in the hydrophobic tip. The figure also shows, at a very low ε_S (=0.1 kcal/mol), the hydrophobicity of surface dominates and the capillary force does not depend much on whether the tip is hydrophobic or hydrophilic. When the surface is strongly hydrophilic (ε_S =2.5 kcal/mol), the capillary force is again dominated by the surface, not quite dependent on the tip hydrophilcity. The force difference between the hydrophilic and hydrophobic tips becomes maximal near ε_S =1 kcal/mol.
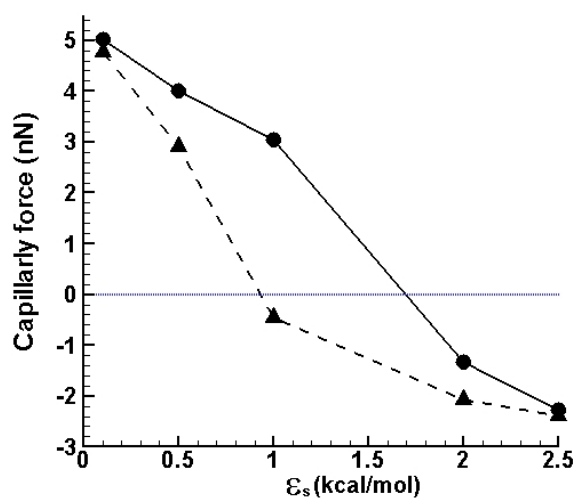

Figure 5: Capillary force as a function of the LJ epsilon parameter of the surface ε_S. Lines represent linear interpolations of data.

4 CONCLUSIONS

We have performed a molecular dynamics simulation of the nanoscale water meniscus formed between an AFM tip and a surface. We examined how the meniscus structure varies as the distance between the tip and surface changes. We obtained the density profile of water for various tip-surface distances and for the tip and surface hydrophilicities. The meniscus periphery obtained from the molecular density profile is not infinitely sharp but instead is fuzzy with a thickness of about half nanometer. Overall, the

meniscus width decreases with an increase in the tip-surface distance. Interestingly, beginning at some tip-surface distance (2.5 nm), the meniscus becomes unstable and its width significantly fluctuates as the tip retracts farther from the surface. Overall, the meniscus width decreases as the tip retracts from the surface, eventually becoming zero at a very long tip-surface distance.

From the structural parameters of the meniscus, we were able to calculate the capillary force by using the Kelvin equation. Such a combined approach gives a force distance curve in reasonable agreement with typical AFM experiment. If the surface is strongly hydrophilic or strongly hydrophobic, the capillary force does not depend much on whether the tip is hydrophilic or hydrophobic. The difference in the capillary force becomes maximal for a moderately hydrophilic surface.

We believe our work will serve as a starting point for further investigation of the nanoscale meniscus and force at the molecular level. For example, a combination of the current MD with the density functional theory [9] should give a more accurate estimate of the capillary force.

REFERENCES

[1] J. N. Israelachvili, "Intermolecular and Surface Science", 2nd edition, Academic Press, 1991

[2] C. A. Mirkin, ACS Nano 1, 79, 2007.

[3] J. Jang, J. Sung, and G. C. Schatz, J. Phys. C. 111, 4648, 2007.

[4] J. Jang, M. Yang, and G. C. Schatz, J. Chem. Phys. 126, 174705, 2007.

[5] W. L. Jorgensen, J. Chandrasekhar, J. D. Madura, R. W. Impey, and M. L. Klein; J. Chem. Phys. 79, 926, 1983.

[6] M. P. Allen and D. J. Tildesley, Computer Simulation of Liquids, Clarendon Press, 1987.

[7] T. Darden, D. York, and L. Pederson, J. Chem. Phys. 98, 10089, 1993.

[8] R. Kubo, M. Toda, and N. Hashitsume, "Statistical Physics II: Nonequilibrium Statistical Mechanics" 2nd Ed., Springer, 1991.

[9] P. B. Paramonov and S. F. Lyuksyutov, J. Chem. Phys. 123, 084705, 2005.